Controlling Synthesis and Characterization of Micron-Sized PNIPAM Microgels with Tailored Morphologies.

ARTICLE *in* LANGMUIR · JULY 2013

Impact Factor: 4.46 · DOI: 10.1021/la402062t · Source: PubMed

3 AUTHORS:

To Ngai
The Chinese University of Hong Kong
94 PUBLICATIONS **1,304** CITATIONS
SEE PROFILE

Manhin Kwok,
The Chinese University of Hong Kong
2 PUBLICATIONS **17** CITATIONS
SEE PROFILE

Zifu Li
Georgia Institute of Technology
25 PUBLICATIONS **372** CITATIONS
SEE PROFILE

Langmuir

Article

pubs.acs.org/Langmuir

Controlling the Synthesis and Characterization of Micrometer-Sized PNIPAM Microgels with Tailored Morphologies

Man-hin Kwok, Zifu Li, and To Ngai*

Department of Chemistry, The Chinese University of Hong Kong, Shatin, N. T. Hong Kong

ABSTRACT: This Article presents the controlling synthesis and characterization of micrometer-sized, multiresponsive poly(*N*-isopropylacrylamide-*co*-methacrylic acid) (PNIPAM-MAA) microgel particles. By combining semibatch and temperature-programmed surfactant-free precipitation polymerization, we have successfully developed a novel approach to the preparation of temperature- and pH-responsive PNIPAM microgels with a dense-shell (DS), dense-core (DC), or homogeneous (HOMO) structure. We then investigated the interaction between the synthesized microgels and some fluorescent dye molecules using confocal laser scanning microscopy (CLSM). Our results have qualitatively revealed that the cross-linkers and the functional carboxylic groups (−COOH) could be homogeneously distributed, predominately localized inside the core, or concentrated near the surface of the synthesized microgels. Moreover, pH-responsive swelling behaviors of the microgels were investigated and discussed with titration and CLSM data. We found that the swelling capability is strongly dependent on the morphology of the PNIPAM microgel. Besides the absorption of fluorescent molecules, the synthesized microgels also showed a strong affinity for fluorescently labeled polypeptide, even at a relatively high salt concentration.

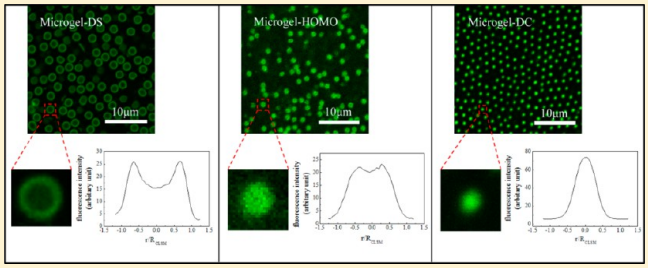

INTRODUCTION

Microgels are colloidal particles that have attracted much attention in soft matter research. They are cross-linked networks of polymer chains swollen with a solvent, such as a normal bulk gel. The microgel particles exhibit a fully reversible conformational transition in response to changing solvent quality, which may be affected by a number of external stimuli such as temperature, pH, and ionic strength.[1] During this kind of transition, the microgel will adopt a more compact conformation in order to minimize polymer−solvent interactions, returning to its original conformation only when solvent conditions become more favorable. Numerous studies have illustrated the applicability of microgels in many different areas, such as wound repair, catalysts, functional membranes, and drug delivery.[2−4] One of the most studied microgel systems is composed of environmentally responsive polymer poly(*N*-isopropylacrylamide) (PNIPAM), which was first reported by Pelton and Chibante in 1986.[5] The PNIPAM microgel is able to undergo a volume-phase transition (VPT) at around 32 °C.[6] At temperatures below 32 °C, the microgels are hydrophilic and in a highly swollen state in water. However, when the temperature is raised to above 32 °C, the microgels become hydrophobic, and they expel their water content and shrink because of the formation of hydrogen bonds within the polymeric structure.[7] By incorporating ionizable functional groups such as acrylic acid (AAc) or methacrylic acid (MAA) as comonomers, one can synthesize ionic microgels that respond not only to temperature but also to pH and ionic strength.[8,9] These adjustable properties make microgel particles desirable for many applications.[10,11]

PNIPAM-based microgel particles are usually prepared by precipitation polymerization. Generally, in the presence of surfactant such as sodium dodecyl sulfate (SDS), the hydrodynamic diameter of the PNIPAM microgels prepared by emulsion polymerization is smaller than 300 nm.[12] However, there is a problem with completely removing the surfactants from the resulting microgel particles. Even if there is no surfactant added, the size of PNIPAM microgels prepared by precipitation polymerization is limited to around 1000 nm, which may not offer the possibility to study the physical properties of individual microgel particles using conventional optical microscopy. Lyon and his colleagues have recently developed a temperature-programmed surfactant-free precipitation polymerization technique in which PNIPAM-*co*-AAc microgels with a hydrodynamic diameter of about 2.5 μm could be produced.[13] However, the morphology of the resulting microgel is limited by the reactivity differences of the monomers.

Recent studies have also focused on understanding how the functional comonomer distribution affects the physicochemical properties of microgel particles.[14−16] PNIPAM-*co*-MAA microgels prepared by conventional precipitation polymerization usually have a nonuniform structure with a highly cross-linked core surrounded by a shell of dangling polymer chains. This is because the reactivity of the cross-linker, such as *N*,*N*′-methylene(bisacrylamide) (MBA) and comonomer MAA, is

Received: May 30, 2013
Revised: July 5, 2013
Published: July 8, 2013

dx.doi.org/10.1021/la402062t | *Langmuir* 2013, 29, 9581−9591

much greater than that of NIPAM monomers, with reactivity ratios of 2.659 and 2.064, respectively.[17] In this way, the cross-linkers and the functional −COOH groups will be mainly located in the core of the resulting particles after batch synthesis.[18,19] Several reports, however, have indicated that the distribution of the cross-link density and functional groups has a profound effect on the properties of the microgels, such as swelling, optical properties, and their interaction with functional molecules including polymers, DNA, and enzymes.[20] From this perspective, the development of new synthesis approaches for improving the control of cross-linker and functional group distributions in microgels is also essential to the design of more advanced microgel structures for specific applications.

To control the carboxylic functional group distribution, Hoare and co-workers have applied semibatch synthesis to obtain thermoresponsive microgels with different functional group distributions.[21] The microgels were well characterized by transmission electron microscopy (TEM). However, the images were obtained in the dried, collapse state of microgels, and the cross-linking distributions were not well controlled in the synthesis.

Therefore, in this Article, we report a novel synthesis that combines the two mentioned approaches to control the morphologies of the resulting microgels. The syntheses of the microgels were performed in a two-stage approach. A core was first formed, and the shell was constructed on it. Besides controlling the functional group (e.g., −COOH distribution), we also controlled the cross-linker distribution inside the microgel particles. Instead of obtaining conventional scanning electron microscopy (SEM) or TEM images in the dried collapsed state, the large microgels allow characterizations in aqueous solution under fluorescence microscopy. This is very important because the properties and the behaviors of the microgels are strongly dependent on its water content and the interaction with the solvent. Drying of microgels usually results in a flat, collapsed polymer instead of a swollen gel.[22] Therefore, it is beneficial to use optical microscopy for direct inspection in studying the properties of the microgels.[23] Also, fluorescein was used to demonstrate the interaction between the microgels and small molecules, which may relate to the absorption and release of drugs in potential drug delivery applications. We showed that microgels with various morphologies interact with dye molecules differently at different pH values. Also, the pH-responsive swelling properties of the microgels are discussed.

EXPERIMENTAL SECTION

Materials. *N*-Isopropylacrylamide (NIPAM, Fluka) was recrystallized using a 1:1 toluene/*n*-hexane mixture twice. *N*,*N*′-Methylene-bisacrylamide (MBA, Fluka) was recrystallized by using methanol. Methacrylic acid (MAA, Merck) was vacuum distilled at around 50 °C in order to remove the stabilizer. Potassium persulfate (KPS, Merck), FITC-labeled poly-L-lysine (M_w = 68 300 g/mol, Sigma-Aldrich), and fluorescent sodium salt (FSS, Sigma Aldrich) were used as received. Milli-Q deionized water was used in all experiments.

Preparation of PNIPAM-*co*-MAA Microgels. We have synthesized three types of micrometer-sized microgels with different spatial distributions of the −COOH functional group and cross-linker.

PNIPAM-co-MAA microgels with a Dense Functionalized Core (Microgel-DC). NIPAM monomer (0.6 g), MBA (0.032 g), and MAA (0.15 mL) were dissolved in 55 mL of deionized water and filtered to remove any solid impurities. The solution was then transferred to a 100 mL round-bottomed flask, and 16 μL of 0.75 M sulfuric acid was also added to the solution. To remove the dissolved oxygen, we purged the sample with nitrogen gas and stirred the solution in a 40 °C water bath for 1 h. Then, 0.055 g of KPS was dissolved in 1 mL of deionized water and added to the reaction vessel with a syringe to initiating the polymerization. When the reaction mixture started to turn opalescent, the temperature was ramped to 60 °C in 1 h. Then, 6 mL of a solution containing an extra 0.6 g of NIPAM was added with a syringe pump in 1 h. Finally, the reaction mixture was stirred for 2 more hours at 60 °C.

PNIPAM-co-MAA Microgels with a Dense Functionalized Shell (Microgel-DS). Similar to that of microgel-DC synthesis, the monomer solution was prepared. However, only 0.6 g of NIPAM monomer was dissolved to form the solution. After purging the solution of oxygen, we dissolved 0.055 g of KPS in 1 mL of deionized water and added it to the reaction vessel with a syringe to initiate the polymerization. When the reaction mixture started to turn opalescent, the temperature was ramped to 60 °C in 1 h. At the same time, 0.6 g NIPAM, 0.032 g MBA and 0.15 mL of MAA were dissolved in 6 mL DI water. Once the temperature reached 60 °C, the comonomer solution was added in 1 h using a syringe pump. Finally, the reaction mixture was stirred for 2 more hours at 60 °C.

PNIPAM-co-MAA Microgels with Homogeneous Functional Groups (Microgel-HOMO). NIPAM monomer (0.9 g) was dissolved in 55 mL of deionized water and filtered to remove any solid impurities. The removal of dissolved oxygen was done similarly to the previous two syntheses. Then, 0.055 g of KPS was dissolved in 1 mL of deionized water and added to the reaction vessel to initiate the polymerization. Two minutes after the initiation, 6 mL of solution containing 0.3 g of NIPAM, 0.032 g of MBA, and 0.15 mL of MAA was added at a rate of 5 mL/h. When the reaction mixture started to turn opalescent, the temperature was ramped to 60 °C in 1 h. After all of the 6 mL comonomer solution was added, the reaction mixture was stirred for 2 h more at 60 °C.

Preparation of Pure PNIPAM Microgels in the Absence of MAA and/or MBA as a Control (Microgel-R1 and Microgel-R2). Pure microgel-R1 and microgel-R2 as controls were synthesized in the same steps as for microgel-DS. However, MAA was not added in the synthesis of microgel-R1, and both MAA and MBA were not added in the synthesis of microgel-R2.

All of the synthesized microgels were purified by centrifugation so that the unreacted monomers, dissolved polymer chains, and unreacted initiator can be removed. The microgels were purified at a constant maximum centrifugal force of 6000*g* for 1 h. After that, the supernatant was removed and the microgels were redispersed in deionized water by stirring overnight. The centrifugation was repeated four times for each of the samples.

Physical Measurements. *Laser Diffraction Measurement.* A 0.01 M phosphate buffer of pH 2.6 was prepared. The buffer solution was used to fill up the sample chamber of the Coulter LS230 laser diffraction size analyzer. Detectors were aligned and background measurements were made using the provided software. Then microgels samples were added, and the measurements of the particle sizes were performed with the provided software.

Concentration Determination. The mass of a clean glass vial was recorded accurately. After that, about 1 mL of the purified microgel samples was transferred to the glass vial, and the total mass of it was measured carefully. Then all of the water was evaporated. After the vial was cooled to room temperature, the total mass of the residue and the vial was measured again. Finally, the concentration of the microgel dispersion was calculated as a weight percentage. The measurement was repeated three times, and the average value was taken.

Determination of MAA Content in Microgels. Typically, 3 mL of a purified microgel sample was added to 20 mL of deionized water. A syringe pump loaded with 0.1 M KOH solution was used to titrate the microgel sample. A pH meter was calibrated and inserted into the solution, and a magnetic stirrer was also added to stir the solution throughout the whole titration process. Before the titration, 0.07 mL of a 1 M HCl solution was added to the diluted microgel solution to ensure that all of the COOH groups in the microgels are protonated. The pH value of the resulting solution was 2.42. Then, 0.1, 0.05, and 0.025 mL portions of a 0.1 M KOH solution were added to the microgel dispersion. The pH values were recorded when the values

dx.doi.org/10.1021/la402062t | *Langmuir* 2013, 29, 9581−9591

became stable. Finally, the MAA content was calculated by using the weight concentration of the samples and the titration results.

Measurement the pH as a Function of the Size of the Microgel Particles. A 0.9 mL portion of a 0.6 wt %/wt microgel solution (except for microgel-DC, the images were taken after centrifugation.) was prepared by diluting the purified microgel with deionized water. Then, 0.05 mL of a 0.3 mg/mL fluorescein sodium salt (FSS) was added to the microgel solution to label the microgels. Following that, different amounts of 0.089 M citric acid and 0.178 M disodium hydrogen phosphate solution were added to the microgel solution. In this way, the pH value of the resulting microgel solutions was adjusted to range from pH 2 to 8. Extra KOH solution was added to tune the pH values to a more alkaline condition. Confocal laser scanning microscopy (CLSM) images of the microgel samples were taken with a Nikon Eclipse Ti inverted microscope (Nikon, Japan). A laser with wavelength of 488 nm was used to excite the fluorescent sodium salt (FSS). A 60×, NA = 1.49 oil-immersion objective was used. The images of the microgel were taken at different pH values. For each pH value, more than 30 microgel particles were counted to obtain the average diameters of the microgel particles.

Absorption of Poly-L-lysine. PBS buffer was prepared with a commercial PBS tablet (Sigma-Aldrich). Then 0.5 mL of prepared PBS buffer, 0.48 mL of purified microgels, and 0.02 mL of 1 mg/mL poly-L-lysine were mixed together. The CLSM was carried out with the microscope mentioned above.

RESULTS AND DISCUSSION

Synthesis of Microgels with Different Morphologies. Figure 1 schematically illustrates the synthesis steps for the preparation of the three microgels with different morphologies. All of them combined semibatch and a modified temperature-programmed synthesis based on normal surfactant-free precipitation polymerization. The pH values of all of the resulting microgel dispersions were around 4, and they were milky gray solutions.

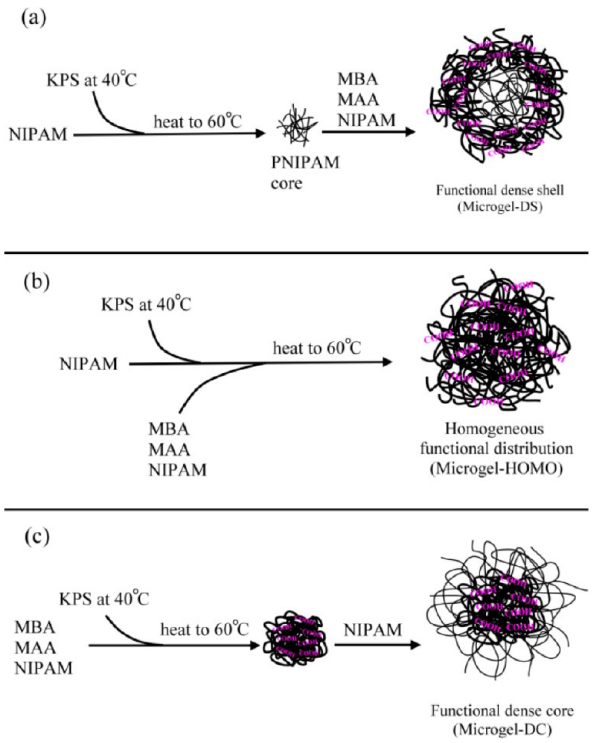

Figure 1. Schematic illustration of the syntheses of three micrometer-sized PNIPAM-based microgels with different morphologies: (a) PNIPAM-*co*-MAA microgels with dense, functionalized shells (microgel-DS); (b) PNIPAM-*co*-MAA microgels with homogeneous functional groups (microgel-HOMO); and (c) PNIPAM-*co*-MAA microgels with dense, functionalized cores (microgel-DC).

Normally, the hydrodynamic radius (R_h) is used to compare the sizes of microgel particles because it is reliable and able to be easily obtained by laser light scattering experiments. Because the sizes of our microgels are in the micrometer range, we used a laser diffraction analyzer to characterize the synthesized microgels. Some studies have suggested tracking particle trajectories under digital microscopy to calculate the diffusion coefficients of the microgels.[13] It is desirable to note that the synthesized microgels are almost isorefractive with water at high pH values so both digital microscopy and laser diffraction are not applicable in determining the diameter of the particle under alkaline conditions. Therefore, in this work, laser diffraction results were obtained under acidic conditions, and the pH-responsive swelling behavior was determined by labeling the microgels with fluorescent dye under CLSM.

Figure 2 shows the size distribution of the three microgels measured by laser diffraction at pH 2.6. The diameters of

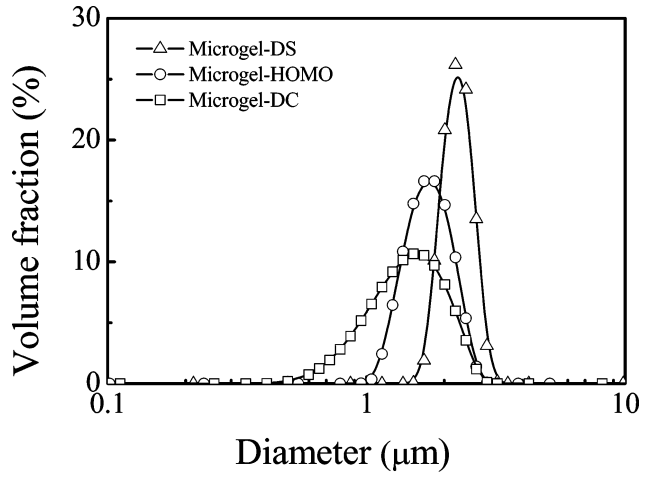

Figure 2. Laser diffraction results of the three synthesized PNIPAM-*co*-MAA microgels with different morphologies measured at pH 2.6.

microgel-DS, microgel-DC, and microgel-HOMO are 2.3, 1.7, and 1.5 μm, respectively, which are 3 to 4 times larger than the microgels obtained from conventional polymerization. Therefore, they are actually 40 times larger than the conventional PNIPAM microgels in terms of volume. Although laser diffraction cannot be applied for all pH values, the results obtained under acidic conditions are important to show that the synthesized microgels are monodisperse. Also, the diameters of the labeled microgels were obtained using CLSM. The CLSM images displayed in Figure 3 show that the diameters of microgel-DS, microgel-HOMO, and microgel-DC are 2.5, 1.75, and 1.88 μm, respectively. All of them are compatible with the corresponding results obtained by the laser diffraction analyzer, especially considering that the microgels are soft, porous, and highly swollen.

The possible reasons for the preparation of such large microgel particles in our approach are illustrated as follows. Surfactant free-emulsion polymerization (SFEP) is commonly used for the preparation of PNIPAM microgels. This can be attributed to the fact that the NIPAM monomer is quite soluble in water whereas the solubility of the polymerized chains in water is low at reaction temperatures above 40 °C. When

dx.doi.org/10.1021/la402062t | *Langmuir* 2013, 29, 9581−9591

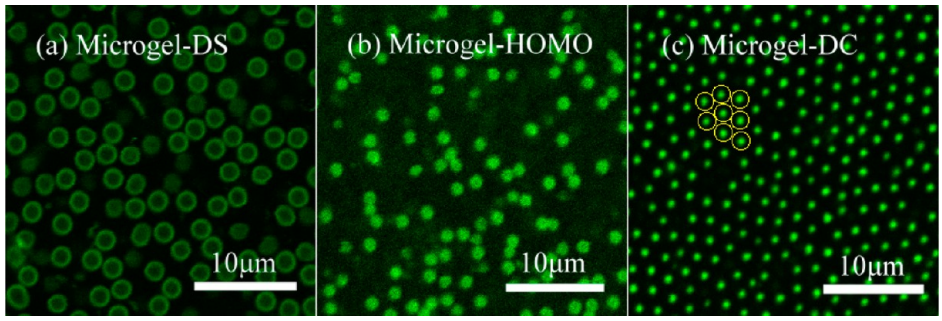

Figure 3. Microgels with different morphologies labeled by FSS under CLSM at pH 2.6. (a) Microgel-DS, (b) microgel-HOMO, and (c) microgel-DC, with the yellow circles indicating the approximate boundaries of the close-packed microgels.

NIPAM monomers polymerize and the polymer chains have grown long enough, the polymer chains will precipitate to form nuclei that grow as individual polymeric particles. This phase-separation process is called nucleation. Note that in the nucleation step these precipitated primary nuclei are not very stable and they may aggregate with each other until the accumulated charge is great enough to stabilize them and prevent them from further aggregation. The nucleation step is crucial to controlling the size and monodispersity of the final microgel particles. Normally, to synthesize larger PNIPAM microgel particles, we need to control the total number of nuclei formed in the nucleation stage of polymerization. It is reasonably assumed that with fewer nuclei and the same amount of monomer much larger microgels can be prepared. To achieve this, we need to lower the stability of the precursor particles. Compared to emulsion polymerization with surfactants, the particles prepared by SFEP are usually larger. This is because in an early stage polymerization the surfactant molecules can stabilize the primary particles so that numerous smaller primary particles can be formed in the initial stage.

In our approach, we modify the conventional SFEP by the incorporation of the semibatch process and a temperature ramp. The initial reaction containing pure NIPAM monomer and persulfate initiators (nucleation) was kept at 40 °C. At this temperature, the persulfate initiators are expected to be decomposed at a much slower rate than at 70 °C. This slow decomposition rate of the initiators likely reduces the oligomeric radical concentration, thereby lowering the abundance of collapsed nuclei. Furthermore, in the nucleation stage, the stability of the formed primary nuclei is mainly contributed by the anionic charge of the persulfate radicals. At lower temperature, the amount of decomposed persulfate was reduced and there is a greater chance for these primary nuclei to aggregate with each other. It further decreases the number of nuclei formed in the nucleation step. As the reaction continuously proceeds and monomer is consumed, the propagation rate decreases. To compensate for this decrease in the propagation rate, the reaction temperature is ramped gradually up from 40 to 60 °C. This ramp increases the propagation rate and also the decomposition rate of the initiator, leading to the generation of more radicals. However, it is worth pointing out that if the temperature ramp rate is doubled, the ramp will be too fast and a second nucleation may occur because there will be a large number of newly initiated chains. After about 60 min of polymerization, the temperature of the reaction mixture reaches 60 °C, and the majority of monomers were likely converted to oligomeric radicals, nuclei, and primary particles. Under this condition, the growth of the particles comes after the nucleation stage, which is achieved by monomer addition, nuclei absorption, and nuclei aggregation. Therefore, the growth on the particles is more favorable than nucleation because of the much lower monomer concentration. In short, starting the nucleation stage at a lower temperature leads to the growth of fewer large self-cross-linked microgel cores, which then serve as a seed for subsequent polymerization to yield the resulting micrometer-sized microgel particles in our approach.[24]

For the synthesis of microgels with homogeneous morphology (microgel-HOMO, Figure 1b), comonomers of MAA and MBA were added continuously during the whole particle-formation process. It is important to apply a small delay of around 2 min before the addition of the comonomers in the preparation of larger microgels because if the comonomers are added before the nucleation process occurs then some of the MAA monomers will be deprotonated and will provide much more stabilization to the precursor particles as they polymerize. The resultant microgel will have a diameter of only around 900 nm. For the synthesis of microgels with functionalized dense cores (microgel-DC, Figure 1c), the presence of MAA in the initial reaction mixture could not be avoided. Therefore, a small amount of sulfuric acid was added to the reaction mixture to suppress the dissociation of the MAA. The resulting pH of the solution is around 3. We had tried an even lower pH value in order to get a larger diameter. However, an excessive amount of aggregate was formed during the temperature ramp. Also, we had optimized the rate and the time of the addition of monomer in the shell-construction stage. If the monomer for shell construction is added in 40 min or less, then the monomer addition will be too fast and serious second nucleation will occur. If the NIPAM monomer is added too slowly (3 h), then the growing polymer chain will have a much greater chance of being terminated and the efficiency of the shell construction will be decreased. Finally, for the preparation of microgels with a pure PNIPAM core and a functionalized dense shell (microgel-DS, Figure 1a), only NIPAM monomer was present in the initial reaction mixture. The precursor particles are stabilized only by the anionic initiator. Therefore, the size of the dense-shell loose-core microgel is a bit larger than those of dense-core and homogeneous structured microgels. Similar to the synthesis of microgel-DC, the temperature ramp rate and addition rate of comonomers were optimized to reduce the chance of second nucleation. Also, the nucleation temperature of 40 °C is chosen because if the temperature is further lowered to 37.5 °C then the oligomeric polymer chains will not be able to precipitate from the solution.

dx.doi.org/10.1021/la402062t | *Langmuir* 2013, 29, 9581−9591

Titration of Microgels with Different Morphologies. To characterize the pH-responsive property, the most direct and simple method is through titration. MAA is a weak organic acid with a pK_a value of 4.8. For all three synthesized microgels, the total amounts of each monomer were the same and the amount of MAA was 1.3 mmol/g monomer. The microgel recovery of all three microgel samples was only around 65% because in the synthesis many polymer chains will also be formed in the reaction mixture. These chains are not covalently linked to the growing microgels, and they are removed during the purification process. Therefore, if these chains contain less pMAA than the microgels do, then the % MAA incorporation might exceed 100% as shown in Table 1.

Table 1. MAA Contents of the Microgels Measured by Titration with 0.1 M KOH

	MAA content mmol −COOH/g microgel	% MAA incorporation
microgel-DS	1.8 ± 0.1	135
microgel-HOMO	1.7 ± 0.1	130
microgel-DC	1.4 ± 0.1	104

The synthesized microgels also exhibit a significant polyelectrolyte effect because the carboxylic acid groups in the polymeric networks in the microgels are quite close to each other.[25] The deprotonation of them significantly changes the environment of the adjacent carboxylic groups. Initially, the carboxylic groups form hydrogen bonds with each other. When some of them are deprotonated to carboxylate anions, they will form stronger hydrogen bonds with the remaining carboxylic groups. This lowers the free energy of the system and prevents the bonds from dissociating. As a result, more energy is required to deprotonate the carboxylic groups, and the effective pK_a of the microgels will increase. Therefore, the increase in the effective pK_a indicates the carboxylic clustering effect, and the denser the carboxylic groups, the larger the increase in the effective pK_a. Because the same functional comonomer was used for the synthesis of all three microgel samples, the densities of −COOH groups in the polymeric networks among the three microgels with different morphologies can be compared by their effective pK_a results.

From Figure 4, we can see that the resulting pK_a values of microgels are very different. Microgel-HOMO and microgel-DS have very similar MAA content. Their effective pK_a values at a small degree of ionization (α) are both around 5.5, which is very similar to the results obtained from small PNIPAM-*co*-MAA microgels as reported by Hoare and co-workers.[24] This is a bit higher than the pK_a value of monomer MAA. It is caused by the hydrogen bonds formed by the protonated carboxylic groups in the microgel networks. When α increases, both of them are increased, but the slope of microgel-DS is significantly larger than that of microgel-HOMO and the effective pK_a value of microgel-DS even reaches 7 at high α. As a result, we expect that there is a higher clustering effect in microgel-DS, which indicates a denser distribution of carboxylic groups in the microgels. For similar overall MAA content (shown in Table 1), it is expected that microgel-HOMO will have a more even distribution of −COOH.

For microgel-DC, the effect is even more obvious. The titration curves shows that the MAA content of microgel-DC is around 80% compared to that of the other two microgel

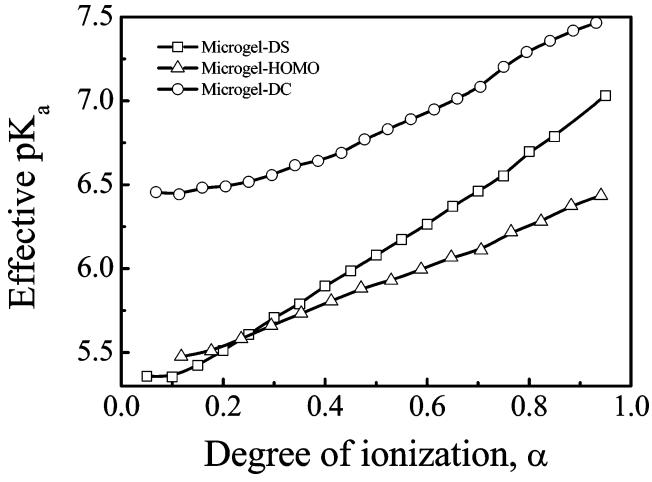

Figure 4. Effective pK_a of the three synthesized PNIPAM-*co*-MAA microgels with different morphologies obtained from the titration results.

samples. However, with less pMAA in the dense-core microgel, the effective pK_a value at low α is already significantly higher than for the other two samples. It shows that the distribution of −COOH groups in microgel-DC might be very dense. As α increased, the effective pK_a value of microgel-DC increased to almost 7.5. It is much larger than the original pK_a value of MAA, indicating a very strong polyelectrolyte effect inside the microgel.

Both dense-shell and dense-core microgels show relatively denser distributions of −COOH groups compared to microgel-HOMO. However, to account for the difference between the effective pK_a values of microgel-DS and microgel-DC, the differences in the synthesis steps are considered. The core of the microgel-DC was synthesized by batch synthesis whereas the functionalized shell of microgel-DS was synthesized by a continuous feed of comonomer solution in 1 h. Therefore, the MAA monomer concentration was kept nearly constant throughout the formation of the shell of microgel-DS. Because the reactivity of MAA and MBA should be a few times greater than that of NIPAM, the synthesized core of microgel-DC should already possess an uneven distribution of comonomers. As a result, the functionalized shell of microgel-DS should be considerably more homogeneous than the functionalized, dense core of the microgel, leading to the difference in the effective pK_a values.

Qualitative Characterization of the Cross-Linker and −COOH Functional Group Distributions. Before the three synthesized microgels were characterized, the interaction between the microgels and the anionic fluorescent dye (fluorescein sodium salt, FSS) was thoroughly investigated. FSS is a dianion, and it can be present in different forms depending on the pH of the solution. The pK_{a1}, pK_{a2}, and pK_{a3} values of FSS are 2.27, 4.32, and 6.50, respectively.[26] It was found that besides labeling the microgels under the CLSM, FSS is also capable of labeling specific parts of the microgels at different pH values. Combined with the unusually large sizes of synthesized PNIPAM microgels, the internal structures of the microgels are characterized.

To study the origin of the absorption and release of the fluorescent dye molecules, two more microgels were prepared by exactly the same procedures as used for microgel-DS (Figure 1a). They are microgel-R1 and microgel-R2, and the details are

dx.doi.org/10.1021/la402062t | *Langmuir* 2013, 29, 9581−9591

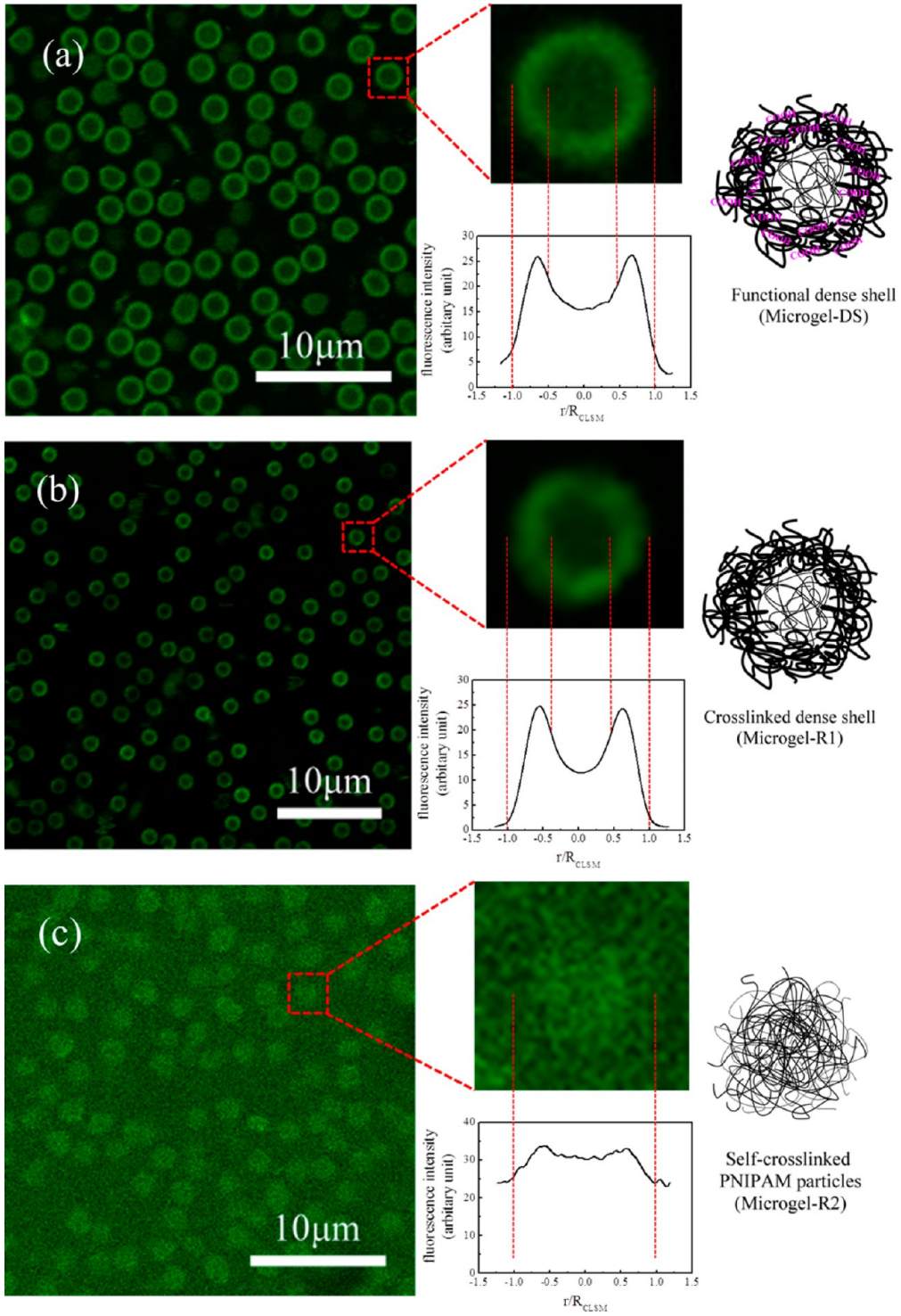

Figure 5. CLSM images of microgels with different comonomer contents at pH 3 and the average fluorescence intensity profiles of them. R_{CLSM} was defined as the radius of the microgel particle under CLSM: (a) microgel-DS, (b) microgel-R1, and (c) microgel-R2.

described in the Experimental Section. However, it is important to note that MAA monomer was not added during the synthesis of microgel-R1 and neither the MAA nor the MBA monomer was added to prepare microgel-R2. That means that neither of these reference microgels contains the functional COOH groups. The diameter of microgel-R1 and microgel-R2 is around 2.2 μm, which is very similar to that of microgel-DS. Microgel-R1 is also considered to possess a dense-shell, loose-core structure, which was similar to that of microgel-DS because of the addition of cross-linker in the second stage of the synthesis. Frisken and co-workers have shown that NIPAM can be polymerized and self-cross-linked to form microgel particles in the absence of cross-linker.[24] Microgel-R2 is basically pure PNIPAM microgel with self-cross-linking only, so the polymeric structure of the microgel should be considerably looser compared to that of other samples.

As can be seen from the CLSM images shown in Figure 5, the FSS dye was effectively absorbed by microgel-DS and

dx.doi.org/10.1021/la402062t | *Langmuir* 2013, 29, 9581−9591

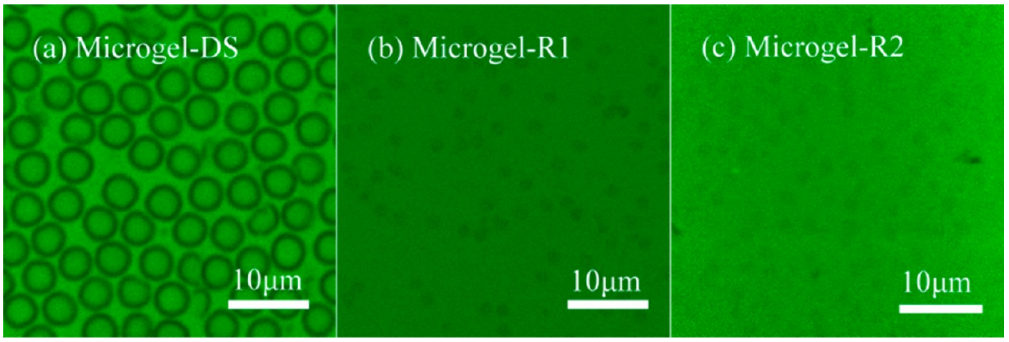

Figure 6. CLSM images of microgels with different comonomer contents at pH 10: (a) microgel-DS, (b) microgel-R1, and (c) microgel-R2.

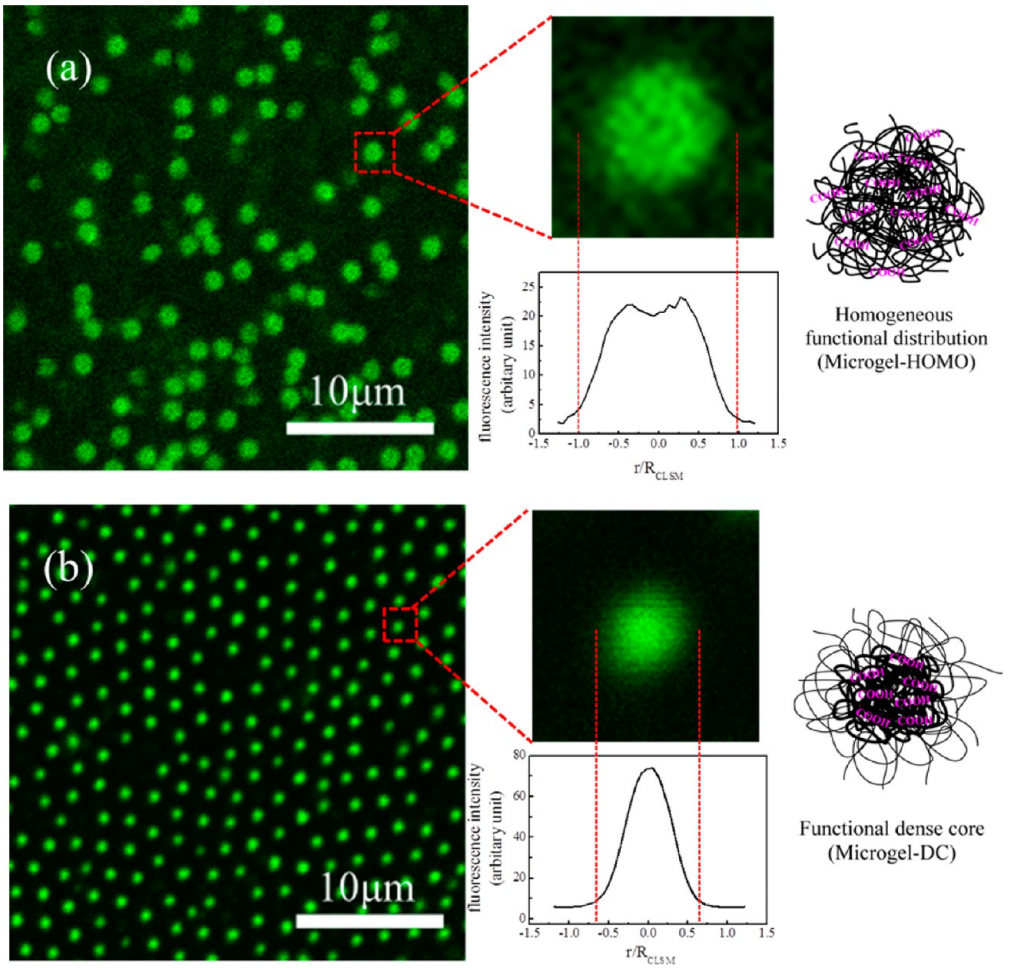

Figure 7. CLSM images of microgels with different morphologies at pH 3 and the average fluorescence intensity profiles of them. (a) microgel-HOMO and (b) microgel-DC.

microgel-R1 under acidic conditions. The labeled microgels are able to be observed clearly. However, the FSS dye is absorbed only weakly by microgel-R2. The fluorescence intensity of the microgel is very similar to that of the aqueous background, and the outlines of the microgel particles are just barely seen. At pH 3, the majority of the FSS dye is in its neutral form. Also, the −COOH groups on the microgels are protonated under acidic conditions. Therefore, the absorption and binding of the FSS molecules by the microgels are presumably caused by the formation of hydrogen bonds between the −COOH groups or amide groups in the microgels and the benzoic acid groups and phenolic hydroxyl groups on the FSS molecules. It was interesting to see that the fluorescence intensity profiles of microgel-DS and microgel-R1 were almost the same, indicating that the presence of pMAA in the microgel does not strongly affect the absorption of the dye. For both of them, the dye is mainly located at the periphery of the particles. Although microgel-R2 absorbs the dye only weakly, the distribution of dye inside the microgel is much more homogeneous compared to that of microgel-DS and microgel-R1. Therefore, it is obvious that the absorption of FSS molecules by the microgel at low pH values is strongly dependent on the cross-linker density of the microgel. This allows the qualitative characterization of the cross-linker distribution of the microgel. This

dx.doi.org/10.1021/la402062t | *Langmuir* 2013, 29, 9581−9591

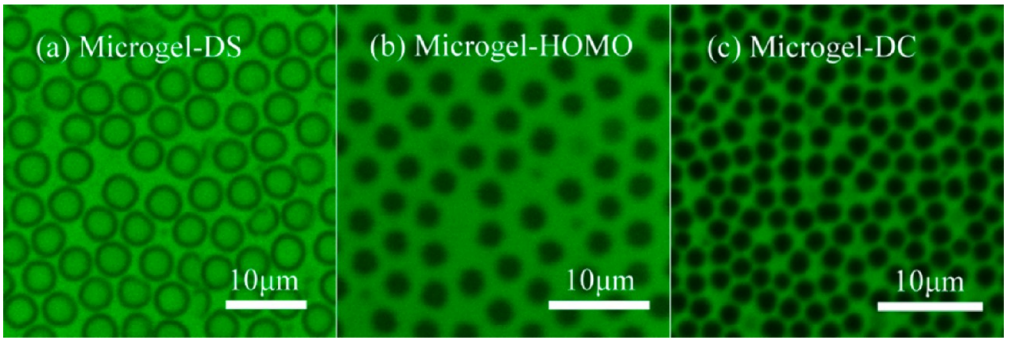

Figure 8. CLSM images of microgels with different morphologies at pH 10. (a) Microgel-DS, (b) microgel-HOMO, and (c) microgel-DC.

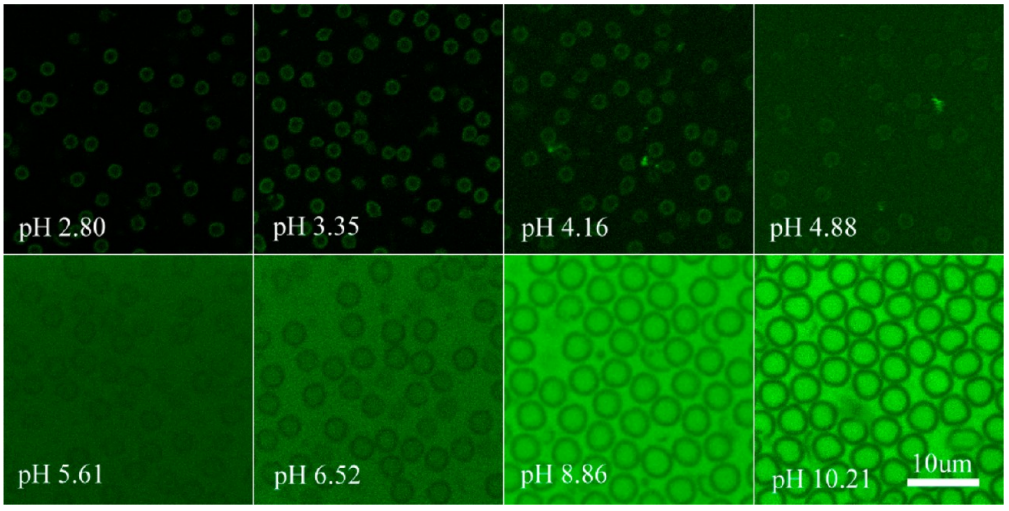

Figure 9. CLSM images of microgel-DS at different pH values on the same scale.

phenomenon may be caused by the formation of multiple hydrogen bonds between the microgel and the dye molecules. The fluorescent molecule possesses multiple sites ready for hydrogen bonding. Therefore, if the polymeric network is denser, the dye molecules will have a greater chance of forming multiple hydrogen bonds with the microgel and being locked in the network, resulting in stronger binding.

Under alkaline conditions, the CLSM image of microgel-DS in Figure 6 shows that the periphery of the microgel is dark and the outlines of the particles are shown clearly. There is only a small amount of fluorescent dye located on the shell of the microgel. However, the CLSM images of microgel-R1 and microgel-R2 are very similar to each other. Microgel-R1 and microgel-R2 leave only some blurred, dark circular shadows.

At pH 10, the −COOH groups in microgel-DS are all deprotonated and the FSS molecules are in the dianion form. Therefore, it is reasonable to expect that the electrostatic repulsion between them likely expelled most of the FSS out of the periphery of the particles. Microgel-R1 and microgel-R2, which do not contain any −COOH groups in the microgels, are essentially invisible in the CLSM images. The blurred shadows are present because microgel-R1 and microgel-R2 actually possess a small amount of negative charge originating from the persulfate initiators. Because the amount of negative charge is very small, the anionic fluorescent dye was repelled weakly, leaving the blurred dark images. Therefore, the exclusion of FSS molecules by the microgel under alkaline conditions is proven to be dependent on the distribution of −COOH groups in the microgel. This allows the qualitative characterization of the carboxylic group distribution of microgel-DS.

The fluorescence intensity profiles of microgels with three different morphologies are very different from each other. As shown in Figure 5a, there are two peaks in the intensity profile of microgel-DS, indicating that more dye was absorbed at the periphery of the microgel. Therefore, it can be confirmed that the cross-linker density in the shell was higher than that in the core of microgel-DS. The CLSM image of microgel-HOMO shows that the dye is homogeneously absorbed by the particles (Figure 7a). A broad peak is shown in the intensity profile of microgel-HOMO. In the CLSM image of microgel-DC (Figure 7b), small bright spots are found, and most of them are separated by a constant distance within some hexagonal patterns. It is believed that there must be a loose PNIPAM shell covering each core, although the shells are not effectively labeled by the fluorescent dye. Also, the loose PNIPAM shell should contains negligible amounts of MAA and MBA. Because MAA and MBA reacted faster than NIPAM, most of the MAA and MBA monomers should be consumed in the first-stage core-formation process. The average diameter of microgel-DC is obtained by the separation of the particles in hexagonal packing sites. There is a single sharp peak located in the center of the intensity profile of microgel-DC. Therefore, microgel-DC should possess a highly cross-linked core and the cross-linker density of microgel-HOMO is relatively homogeneous.

Under alkaline conditions, the turbidity of all three synthesized microgel solutions is very low. The solutions of microgel-DS and microgel-HOMO are almost clear because in

dx.doi.org/10.1021/la402062t | *Langmuir* 2013, 29, 9581−9591

the fully swollen state the microgels are isorefractive with water and are unable to be observed with a normal optical microscope. However, in FSS solution, all three samples can be clearly seen. From the exclusion of the fluorescent dye by the microgels, the −COOH-functionalized shell of microgel-DS can be confirmed (Figure 8a). The CLSM images of microgel-HOMO and microgel-DC are quite similar at this pH value (Figure 8). The dye is homogeneously excluded by the two microgels, but small separations always existed between the microgel particles because the nonfunctionalized PNIPAM shell of the microgel-DC particle does not strongly exclude the dye whereas it still separates the particles from each other. The CLSM images indicate that the outermost part of microgel-HOMO may contain slightly fewer −COOH groups. Therefore, to differentiate the distribution of −COOH groups between microgel-HOMO and microgel-DC, the titration results are also essential.

pH-Responsive Property of the Microgels. To investigate the swelling behavior of the synthesized microgels, the laser diffraction technique is not applied. As mentioned before, this is because the microgels are almost isorefractive with water under alkaline conditions. Therefore, the diameters of the microgels are measured by the CLSM images. Although this method cannot represent the size distribution adequately, it is a direct and simple method of visualizing the pH-responsive property of the microgels.

Figure 9 illustrates the pH-responsive swelling process of the microgel-DS with the same scale bar for different pH values. At pH 2.80 and 3.35, the FSS is absorbed and localized in the periphery of the microgel. As explained above, the loading of FSS is mainly controlled via the formation of hydrogen bonds between the −COOH groups and amide groups in the microgels and the benzoic carboxylic or phenolic hydroxyl groups in FSS molecules. When the pH of the solution is increased to around 4, which is the pK_{a2} of FSS, it can be observed that the fluorescence intensity of the background is also increased. This means that the fluorescent dye starts to enter the solution from the microgels. Also, the average diameter of the microgel is increased. Finally, when the pH value reaches 10, the shells of the microgel particles are not fluorescent at all, indicating that no FSS molecules are located on the shell of the microgel-DS. Most of the FSS dye molecules will be electrostatically expelled from the microgels, being releasing into the outer aqueous solution. From the titration data, it is expected that all of the −COOH groups in microgel-DS should be deprotonated at such a high pH value. The microgel reaches its most swollen state, and the average diameter was 4.7 μm, which is extremely large for a PNIPAM-based microgel prepared by precipitation polymerization. The CLSM image is thus capable of providing direct visualization of the change in diameter of the prepared microgels. It is important to note that the absorption and release of FSS by the microgel particles are reversible. That means that by changing the pH value of the microgels, the loading and release of FSS can be reversibly achieved (Figure 9). We thereby demonstrate that the uptake, distribution, and release of these fluorescent dyes can be reversely triggered through solution pH changes.

Figure 10 shows the diameter swelling ratio q_d of the prepared microgels at different pH values. The synthesized microgels show such a responsive property because the pH increase will induce the dissociation of COOH on the polymer network chains, leading to increasing charge density on the network. The increase in ion content of the microgel network

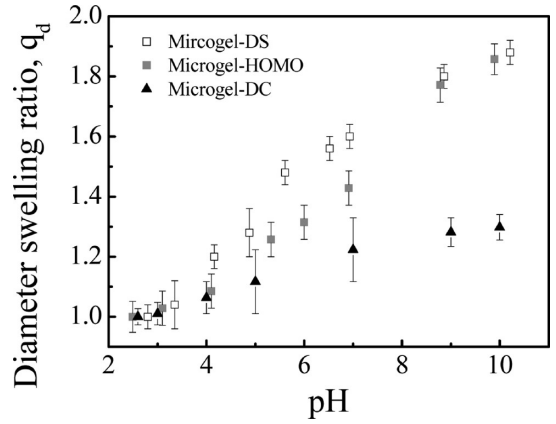

Figure 10. Diameter swelling ratio, q_d, monitored throughout the pH swelling processes of the microgels with different morphologies. The ratios were calculated by dividing the average diameter of the particle by the average diameter in the fully protonated state. The error bars showed the standard deviations of the averaged values.

and hydrophilicity increases the internal osmotic pressure, which induces the swelling of water in the microgel particles. These results confirmed that our synthesized microgel particles were responsive to the pH of the solution. With increasing pH, the COOH groups in the microgel networks are deprotonated so that the electrostatic repulsion and internal osmotic pressure are enhanced. When this repulsion overcomes the attractive forces such as hydrogen bonding and hydrophobic interaction, the microgel network swells.

The swelling profiles of microgel-DS and microgel-HOMO are very similar. The swelling range starts at pH 4 and ends at pH 9. The overall diameter swelling ratios for microgel-DS and microgel-HOMO are 1.88 and 1.86, respectively. Therefore, the volume of microgel under alkaline conditions increases more than 6-fold during the pH swelling process, which is quite large compared to that of small PNIPAM microgels. It is interesting that the swelling ratio of the microgel-DC is significantly smaller than that of the other two microgels with different morphologies. Although its MAA content is a bit lower than that of the other two microgels, it possesses 80% MAA content. Similar results are reported in other studies of small microgels.[21] It is believed that the high cross-linker density near pMAA restricted the swelling of the microgels. We also agree that this would reduce the swelling ratio. A comparison of Figures 7b and 8c shows images of microgel-DC at different pH values. In Figure 7b, which shows concentrated close-packed microgel-DC, the PNIPAM shell is around 350 nm thick. The diameter of the functionalized dense core is around 1.3 μm, and for the microgel under alkaline conditions, the PNIPAM shell is very thin and the diameter of the core is increased to around 2.2 μm. From these data, the diameter swelling ratio of the microgel-DC core is estimated to be 1.7, which is only a little bit smaller than the values for microgel-DS and microgel-HOMO. Therefore, we suggest that the difference in the swelling ratio is mainly dependent on the morphology of the microgel. When microgel-HOMO undergoes pH swelling, obviously the whole microgel particle swells homogeneously. For microgel-DS, when the shell of the microgel swells, the loose core is pulled and stretched by the expanding shell because the core and the shell are chemically linked to each other. Therefore, although the pure PNIPAM core of microgel-DS is not pH-responsive, it swells with the shell. However, if

dx.doi.org/10.1021/la402062t | Langmuir 2013, 29, 9581−9591

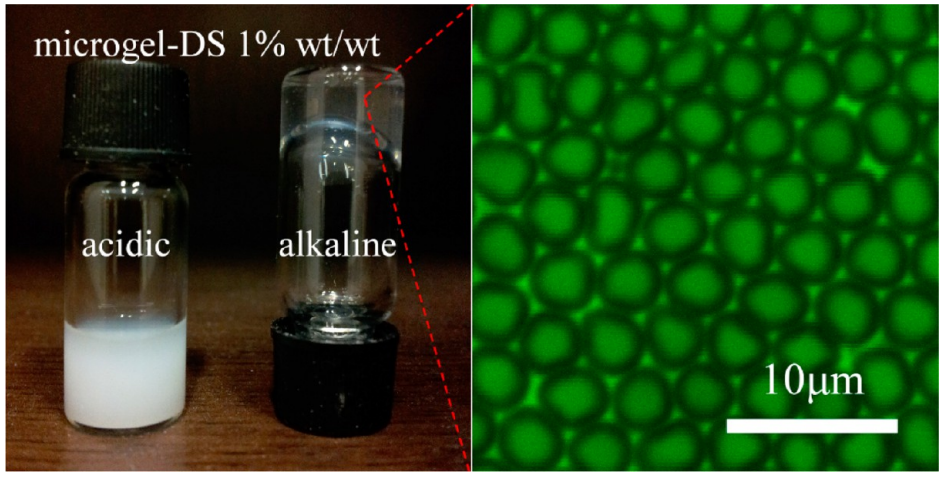

Figure 11. Microgel-DS solution (1 % wt/wt) at pH 2.84 and 10.13. The image on the right-hand side is the confocal image under alkaline conditions.

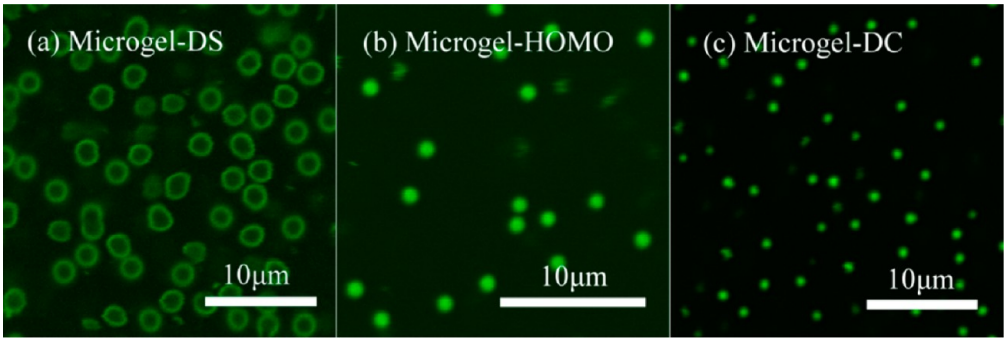

Figure 12. CLSM images of fluorescently labeled poly-L-lysine absorbed by microgels with different morphologies.

the functionalized core of microgel-DC swells, then the loose PNIPAM shell is pushed outward. The shell is thinned as the radius increases whereas the volume of the shell should basically remain unchanged, so when the pH of the microgel-DC solution is increased, only part of the particle swells. As a result, microgel-DC swells less than microgel-DS and microgel-HOMO do.

As mentioned above, the synthesized microgel-DS particles can swell to 6.6 times their original volume. That means that the effective volume fraction of the microgel can also be increased by a factor of 6.6 and exceeds 100% easily when pH of the solution changes from 3 to 10. Figure 11 shows the microgel-DS solution. Under acidic conditions, it is a milky-white solution. When the pH value is increased, the turbidity of the solution decreases rapidly and the solution becomes clear at high pH values. Not only does the turbidity change but also the viscosity of the solution changes during the process because of the change in volume fraction. The vial on the right-hand side of Figure 11 is inverted, and the solution becomes a viscous gel and flows extremely slowly. From the corresponding CLSM image, it can be observed that the microgel particles are squeezed together and deformed. These results show that the synthesized microgels possess strong pH responsiveness.

Absorption of Poly-L-lysine by Microgel Particles. Apart from the absorption of a different fluorescent dye, the absorption of a polypeptide was investigated. The experiments were performed in a dilute PBS buffer to provide a higher salt concentrate than used in the previous dye absorption experiments. The resulting pH values were around 7.0 to 7.3. In this pH range, the carboxylic groups on the three synthesized microgels were almost fully ionized. The commercial fluorescently labeled poly-L-lysine (M_w = 68 300 g/mol) was positively charged at this pH.

Figure 12 shows different distributions of the polypeptide within the microgel particles. The polypeptide was mainly located at the periphery of the dense-shell microgel. At this pH value, the polypeptide and the microgels were carrying opposite charges, so the absorption of polypeptide should be driven by the attraction between the ions, which depends on the distribution of carboxylic groups within the microgels. For homogeneous and dense-core microgels, the labeled polypeptide was absorbed homogeneously and the polypeptide absorbed by the dense-core microgel was more localized. It should be noted that the shell of a dense-core microgel is made of self-cross-linked PNIPAM without any other comonomer. Therefore, the shell of the dense-core microgels may not absorb the dye strongly, and the shells of the particles are invisible under CLSM. Moreover, at such a high salt concentration, all three microgels shrank to almost half of their original diameters. However, the absorption of polypeptide was not affected by the high salt concentration.

CONCLUSIONS

Three types of micrometer-sized PNIPAM-*co*-MAA microgels with different morphologies have been successfully synthesized by a novel temperature-programmed semibatch synthesis. They possess a dense functionalized shell, core, or homogeneous morphology. Their pH responsiveness was studied by

dx.doi.org/10.1021/la402062t | *Langmuir* 2013, 29, 9581−9591

comparing their swelling ratios, and the morphology of the microgel was an important factor in the swelling process. The origin of the absorption and release of fluorescent dye FSS was investigated at different pH values, and it was applied to characterize the internal distribution of cross-linker and pMAA qualitatively. Also, the reversible uptake and release of dye molecules by the microgels demonstrated the potential applicability of microgels in drug-delivery systems. We expect that the synthesized microgels with improved control of functional group distributions would be helpful for making more advanced microgel structures for specific applications.

AUTHOR INFORMATION

Corresponding Author

*E-mail: tongai@cuhk.edu.hk. Tel: +852 − 3943 1222.

Notes

The authors declare no competing financial interest.

ACKNOWLEDGMENTS

The financial support of this work by the Hong Kong Special Administration Region (HKSAR) General Research Fund (CUHK402712, 2130304) and the NSFC/RGC Joint Research Scheme sponsored by the Research Grants Council of Hong Kong and the National Natural Science Foundation of China (N-CUHK454/11, 2900350) is gratefully acknowledged.

REFERENCES

(1) Pelton, R. Temperature-sensitive aqueous microgels. *Adv. Colloid Interface Sci.* **2000**, *85*, 1−33.

(2) Thorne, J. B.; Vine, G. J.; Snowden, M. J. Microgel applications and commercial considerations. *Colloid Polym. Sci.* **2011**, *289*, 625−646.

(3) Saunders, B. R.; Vincent, B. Microgel particles as model colloids: theory, properties and applications. *Adv. Colloid Interface Sci.* **1999**, *80*, 1−25.

(4) Saunders, B. R.; Laajam, N.; Daly, E.; Teow, S.; Hu, X.; Stepto, R. Microgels: from responsive polymer colloids to biomaterials. *Adv. Colloid Interface Sci.* **2009**, *147−48*, 251−262.

(5) Pelton, R. H.; Chibante, P. Preparation of aqueous lattices with N-isopropylacrylamide. *Colloids Surf.* **1986**, *20*, 247−256.

(6) Wu, C. A comparison between the 'coil-to-globule' transition of linear chains and the 'volume phase transition' of spherical microgels. *Polymer* **1998**, *39*, 4609−4619.

(7) Lai, H.; Wu, P. A infrared spectroscopic study on the mechanism of temperature-induced phase transition of concentrated aqueous solutions of poly(N-isopropylacrylamide) and N-isopropylpropionamide. *Polymer* **2010**, *51*, 1404−1412.

(8) Zhou, S. Q.; Chu, B. Synthesis and volume phase transition of poly(methacrylic acid-*co*-*N*-isopropylacrylamide) microgel particles in water. *J. Phys. Chem. B* **1998**, *102*, 1364−1371.

(9) Qiu, X. P.; Kwan, C. M. S.; Wu, C. Laser light scattering study of the formation and structure of poly(*N*-isopropylacrylamide-*co*-acrylic acid) nanoparticles. *Macromolecules* **1997**, *30*, 6090−6094.

(10) Schild, H. G. Poly(N-isopropylacrylamide) - experiment, theory and applicatioN. *Prog. Polym. Sci.* **1992**, *17*, 163−249.

(11) Das, M.; Zhang, H.; Kumacheva, E. Microgels: old materials with new applications. *Annu. Rev. Mater. Res.* **2006**, *36*, 117−142.

(12) Jones, C. D.; Lyon, L. A. Synthesis and characterization of multiresponsive core−shell microgels. *Macromolecules* **2000**, *33*, 8301−8306.

(13) Meng, Z.; Smith, M. H.; Lyon, L. A. Temperature-programmed synthesis of micron-sized multi-responsive microgels. *Colloid Polym. Sci.* **2009**, *287*, 277−285.

(14) Balaceanu, A.; Demco, D. E.; Moeller, M.; Pich, A. Microgel heterogeneous morphology reflected in temperature-induced volume transition and H-1 high-resolution transverse relaxation NMR. The case of poly(N-vinylcaprolactam) microgel. *Macromolecules* **2011**, *44*, 2161−2169.

(15) Dingenouts, N.; Seelenmeyer, S.; Deike, I.; Rosenfeldt, S.; Ballauff, M.; Lindner, P.; Narayanan, T. Analysis of thermosensitive core-shell colloids by small-angle neutron scattering including contrast variation. *Phys. Chem. Chem. Phys.* **2001**, *3*, 1169−1174.

(16) Jones, C. D.; Lyon, L. A. Shell-restricted swelling and core compression in poly(N-isopropylacrylamide) core−shell microgels. *Macromolecules* **2003**, *36*, 1988−1993.

(17) Hoare, T.; McLean, D. Multi-component kinetic modeling for controlling local compositions in thermosensitive polymers. *Macromol. Theory Simul.* **2006**, *15*, 619−632.

(18) Hoare, T.; McLean, D. Kinetic prediction of functional group distributions in thermosensitive microgels. *J. Phys. Chem. B* **2006**, *110*, 20327−20336.

(19) Wu, X.; Pelton, R. H.; Hamielec, a. E.; Woods, D. R.; McPhee, W. The kinetics of poly(N-isopropylacrylamide) microgel latex formation. *Colloid Polym Sci.* **1994**, *272*, 467−477.

(20) Hoare, T.; Pelton, R. Impact of microgel morphology on functionalized microgel-drug interactions. *Langmuir* **2008**, *24*, 1005−1012.

(21) Sheikholeslami, P.; Ewaschuk, C. M.; Ahmed, S. U.; Greenlay, B. a.; Hoare, T. Semi-batch control over functional group distributions in thermoresponsive microgels. *Colloid Polym. Sci.* **2012**, 1181−1192.

(22) Destribats, M.; Lapeyre, V.; Wolfs, M.; Sellier, E.; Leal-Calderon, F.; Ravaine, V.; Schmitt, V. Soft microgels as Pickering emulsion stabilisers: role of particle deformability. *Soft Matter* **2011**, *7*, 7689−7698.

(23) Li, Z.; Kwok, M.-H.; Ngai, T. Preparation of responsive micrometer-sized microgel particles with a highly functionalized shell. *Macromol. Rapid Commun.* **2012**, *33*, 419−25.

(24) Gao, J.; Frisken, B. J. Influence of reaction conditions on the synthesis of self-cross-linked N-isopropylacrylamide microgels. *Langmuir* **2003**, *19*, 5217−5222.

(25) Hoare, T.; Pelton, R. Highly pH and temperature responsive microgels functionalized with vinylacetic acid. *Macromolecules* **2004**, *37*, 2544−2550.

(26) Mota, M. C.; Carvalho, P.; Ramalho, J.; Leite, E. Spectrophotometric analysis of sodium fluorescein aqueous solutions. Determination of molar absorption coefficient. *Int. Ophthalmol.* **1991**, *15*, 321−326.